DOI 10.1007/s11595-012-0564-6

Two-Step Anodization of Maltilayer TiO_2 Nanotube and Its Photocatalytic Activity under UV Light

WANG Xuelai[1], CHEN Rui[2], ZHENG Jun[2], NIE Pan[2], XIE Hao[1], ZHAO Xiujian[1*]

(1.State Key Laboratory of Silicate Materials for Architecture (Wuhan University of Technology), Wuhan 430070, China; 2.School of Material Sciences and Engineering, Wuhan University of Technology, Wuhan 430070, China)

Abstract: A double-layer TiO_2 nanotube arrays were formed by two-step anodization of Ti foils in different electrolytes. First, Ti in 0.5 wt% HF was anodized to form thin nanotube layer. Afterwards a second anodization was conducted in a formamide based electrolyte, which allowed the second layer of nanotube growing directly underneath the first one. From FESEM investigation we found that the thickness of second layer corresponded to the anodization time, the increasing of which would lead to the excessive etching on the first layer. The first layer protected the lower one from fluoride corrosion during anodization process. The double layer TiO_2 nanotube arrays showed no benefit to photodegradation effect in methyl orange degradation experiments.

Key words: double-layer TiO_2 nanotube; anodization; photocatalysis; methyl orange degradation

1 Introduction

Highly ordered TiO_2 nanotube arrays (TNAs) have attracted great attention owing to their potential applications to hydrogen sensing[1, 2], photoelectrochemical water splitting[3], base material in bulk-heterojunctions[4], dye-sensitized solar cells[5,6] and biological material[7-9]. TNAs have been produced by a number of methods, only anodization methods offer superior control to the nanotube structures. In 2001, Gong and co-workers fabricated self-organized, highly uniform TNAs by anodizing Ti in an aqueous dilute HF electrolyte[10]. Considerable efforts indicated that only a limiting layer thickness of approximately 500-600 nm can be obtained in an aqueous dilute HF electrolyte[11]. In order to obtain longer TNAs, Cai and co-workers used buffered electrolytes containing KF or NaF of variable pH value to reduce the chemical dissolution of TiO_2 during anodization[12]. Macak and co-workers produced self-organized regular porous TNAs with 2.5 μm thick in $(NH_4)_2SO_4$ electrolyte containing NH_4F in 2005[13]. Inspired by some organic solvents used in the anodic fabrication of macroporous silicon oxide[14,15], researchers synthesized longer TNAs and smoother nanotube wall in organic electrolytes with higher viscosity. Paulose and co-workers synthesized self-aligned hexagonally closed-packed TNAs over 1000 μm long grown in ethylene glycol electrolyte in 2007[16].

Typically, the nanostructure of TNAs is controlled by the applied voltage, composition, pH values and viscosity of the electrolytes, anodization time and so on. In the present work, multilayer TNAs grown directly by a two-step anodization process was shown and its photocatalytic activities were investigated.

2 Experimental

2.1 Preparation of TNAs

Titanium foils (0.127 mm, 99.7% purity, Aldrich) were degreased by sonication in acetone, ethanol, and deionized water respectively prior to anodization, and finally dried in nitrogen steam. All anodization experiments were conducted at room temperature (25 °C) with magnetic agitation. The Ti foils were subjected to potentiostatic anodization in a two-electrode electrochemical cell connected to a DC power supply (3303C, Taiwan) and current sensor

(Received: Oct. 8, 2011; Accepted: Aug. 19, 2012)

WANG Xuelai (王雪莱): Ph D Candidate; E-mail: shelley4677@gmail.com

*Corresponding author: ZHAO Xiujian(赵修建): Ph D; Prof.; E-mail: opluse@whut.edu.cn

Funded by National Basic Research Program of China (No.2009CB939704)

(Wei Bo Electronics) interfaced with a computer. The samples were first pressed together with a Cu plate and anodized at 20 V in 0.5 wt% HF solution for 20 min. After the anodized Ti foils were rinsed and dried, a second step anodization was performed at 20 V in 0.27 M ammonium fluoride in formamide containing 3% volume water[17] for several minutes. To make comparison, TNAs were directly anodized at 20 V in three different electrolytes with various reaction time: 0.27 M ammonium fluoride in formamide containing 3% water for 5 min, 0.5 wt% HF for 20 min, glycerol and water (50:50 vol%) +0.5 wt% NH_4F[18] for 60 min. The crystallization of TNAs was realized by annealing the as-prepared films at 450 ℃ under ambient air for 2 h.

2.2 Characterization of TNAs

The morphologies of the TNAs were studied using a Hitachi S-4800 field emission scanning electron microscope (FESEM). X-ray diffraction (XRD) patterns were measured on a Rigaku D/MAX-RB X-ray diffraction meter using Cu Kα radiation in the range of 10-80 °. The composition of the TNAs was analyzed with PHI Quantum 2000 X-ray photoelectron spectrum.

2.3 Photocatalytic properties

The photocatalytic degradation of methyl orange (MO) were carried out in a rectangle quartz container equipped with ice water bath. 35 mL of MO solution (2×10^{-5} M) with pH 5 was placed in the container. TNAs were immersed into the MO solution with the working area of 4 cm^2. Ultraviolet light (UV) irradiation on the working electrode from the horizontal direction was carried out by a Newport 300 W arc lamp. The concentrations of the MO solution were measured at every 10 min by UV-Vis absorption spectrums using a SHIMADZU UV-2550 instrument. The detection with UV absorption was performed at 464 nm.

3 Results and discussion

3.1 Morphology of TiO_2 nanotube arrays

After two-step anodization, double-layer, highly ordered TNAs were fabricated on Ti sheet. Fig.1 showed the top view and cross sectional images of the double-layer TNAs prepared with different second anodization time. The first layer of TNAs consisted of approximate 300 nm long tubes formed in 0.5 wt% HF at 20 V for 20 min with a diameter of approximate 100 nm. The second layers were formed in 0.27 M ammonium fluoride in formamide containing 3% volume water with a diameter of approximate 60 nm.

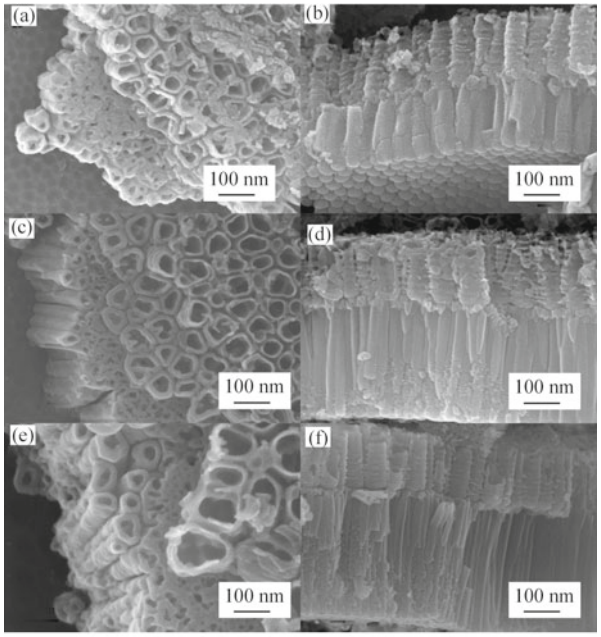

Fig.1 Top view and cross sectional images of double-layer TNAs prepared by two-step anodizing of Ti foil in different electrolytes. The second anodization step in formamide based electrolyte for 2 min (a, b); 3 min (c, d); 4 min (e, f)

The length of the second layers was 300/580/830 nm by applying the anodization time of 2/3/4 min respectively. The second anodization in formamide based electrolyte leaded to longer and smoother tubes. The detailed investigation of the interfaces between the layers showed the second layer of the tubes were formed by etching small channels and/or holes in the bottoms of the first tube layer (Fig.1(e))[19]. The electrolyte permeated through these channels and/or holes into the second layer with the help of the applied voltages. The influence on its photocatalytic property of these small channels and/or holes between the two layers will be discussed in the future work.

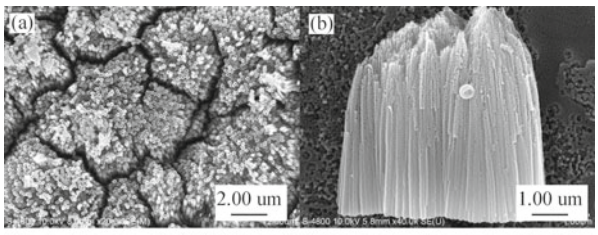

Fig.2 Images of (a)TNAs with the second time anodization for 10 min; (b)TNAs anodized in formamide based electrolyte for 5 min

To obtain more insight into the formation of the second layer, the anodization time was prolonged to 10 min and Ti foil was anodized directly in the formamide based electrolyte. Fig.2(a) showed there was no double-layer structure by prolonging the second

time anodization time to 10 min. The diameter of the tubes was approximately 60 nm in the image, which indicated that the tubes were formed in formamide based electrolyte. It seemed that the first layer formed in HF solution had totally been dissolved during the second anodization process. Fig.2(b) showed the TNAs prepared directly in formamide based electrolyte at 20 V for 5 min consisted of 700 nm long tubes. Without the protection of the first layer, the top part of the TNAs was badly etched while the bottom part was still neatly organized.

3.2 Anodization current analysis

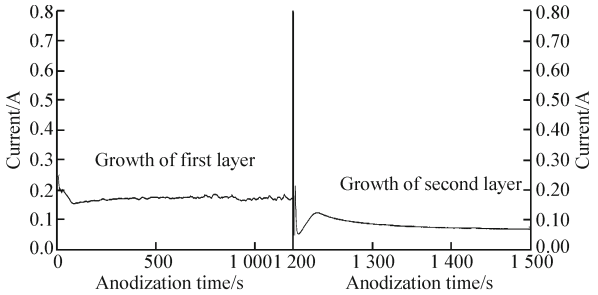

Fig.3 Current transient records for anodization of Ti foil at 20 V during the first growth (in HF solution electrolyte) and the second growth (in formamide based electrolyte)

Fig.3 showed the current transient records during the formation of the first layer in 0.5 wt% HF solution and second layer in formamide based electrolyte at 20 V application voltage. Both processes showed the typical current *vs* time plot. Sharp dip of the current ocurred in the initial period. The current-time transient in a formamide based electrolyte showed much lower current densities than that in the HF solution due to the higher viscosity of the former solution. The decreased dissociation constant (the dissociation constant, D, is proportional to $1/\eta$, where η is the solution viscosity) surpassing pH burst of the electrolyte leaded to the formation of smooth tube wall.

3.3 XRD analysis

Fig.4 showed the XRD patterns of the samples. The TNAs samples were annealed at 450 °C under ambient air for 2 h. Since the TNAs layers were only a few hundreds of nanometers thick, the intensity of the Ti peaks were quite strong, and for some samples it was hard to tell from the peaks of TiO_2. The diffraction peaks, (101), (200), (105) and (211) were indexed to those of the anatase TiO_2 phase, while in sample (d) the diffraction peak (110) was attributed to the rutile TiO_2 phase, which indicated that in sample (d) there was

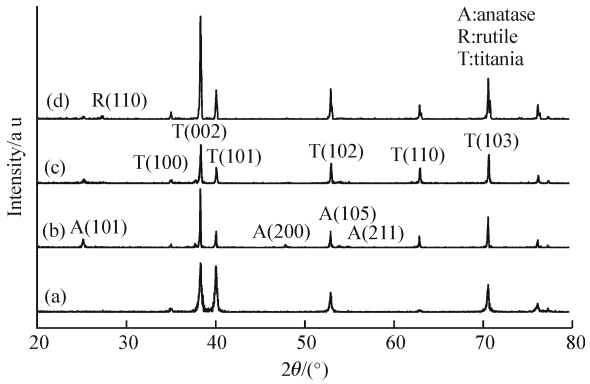

Fig.4 X-ray diffraction patterns of (a)Aldrich Ti foils; (b)TNAs formed in glycerol and water (50:50 vol%) +0.5 wt% NH_4F electrolyte; (c)double-layered TNAs formed first in 0.5 wt% HF solution for 20 min, and then in 0.27 M ammonium fluoride in formamide containing 3% volume water for 5 min; (d)TNAs formed in 0.5 wt% HF solution

crystal phase transfer.

3.4 XPS analysis

According to the XPS survey spectrum (Fig.5(a)) of TNAs calcined at 450 ℃ for 2 h, the sample contained Ti, O, C and N. And binding energies for Ti 2*p*, O 1*s*, C 1*s* and N 1*s* were 458, 531, 285 and 400 eV, respectively. The carbon in this sample could be attributed to the adsorption of organics and dusts. To investigate the elements states in the photocatalyst, we sputtered the sample with Ar^+.

Fig.5(b) showed the high-resolution XPS spectra of the Ti 2*p* of the TNAs before and after Ar^+ sputtering. Deconvolution of the Ti 2*p* 1/2 and Ti 2*p* 3/2 spectrum revealed six components at 464.8, 462.6, 460.8, 459.2, 457.2 and 455.3 eV. The typical binding energy of Ti 2*p* 2/3 peak was 459.7 eV. The new peaks appeared after Ar^+ sputtering with lower binding energies and it proved the formation of low state Ti. The Ar^+ sputtering could reduce Ti^{4+} species into Ti^{3+} and even Ti^{2+} species.

Deconvolution of the O 1*s* spectrum was shown in Fig.5(c). The binding energy values of the individual components were 530.0 eV (Ti-O) and 531.3 eV (Ti-OH), 532.5 eV (Ti-OH_2), in agreement with previous work[20]. After Ar^+ sputtering, all the peaks showed a red shift of 0.5 eV.

There was only one peak before sputtering at 399.8 eV which could be assigned to molecular N_2 or NH_3 chemisorbed onto TiO_2[21]. After sputtering, the peak totally disappeared. Since the anodization electrolyte contains NH_4F, it was not difficult to understand the source of surface N element.

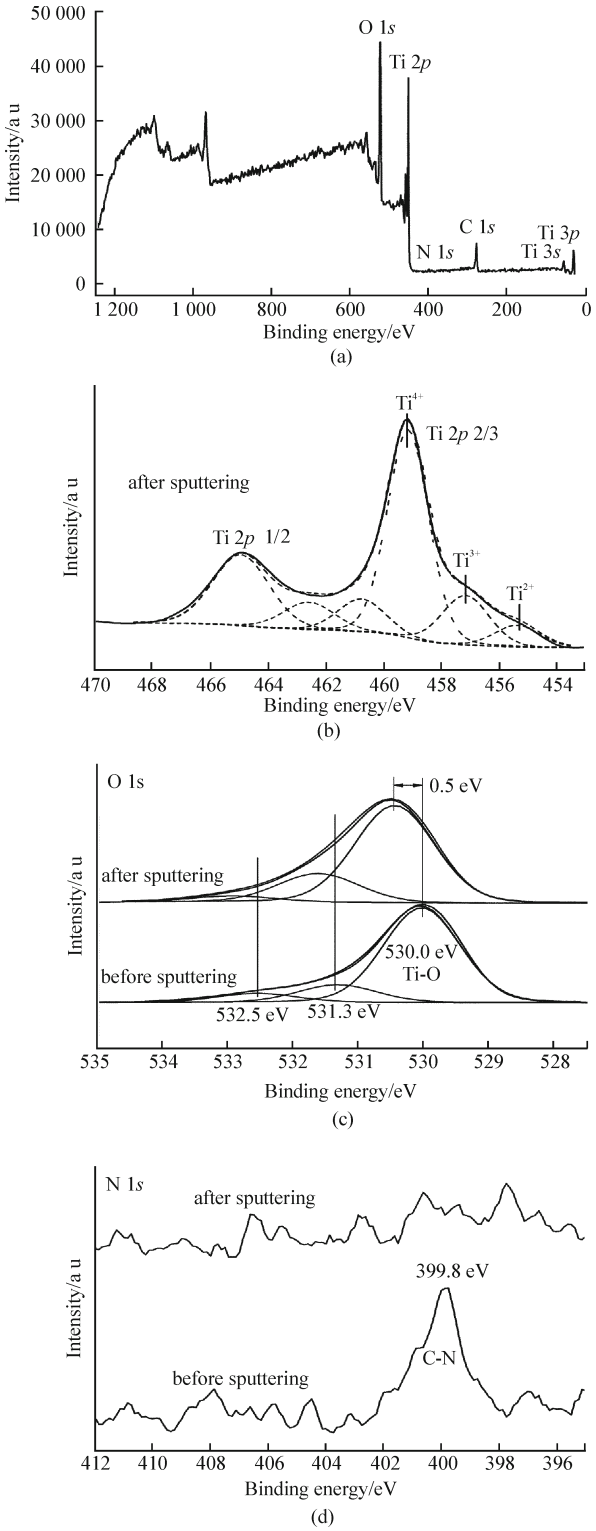

Fig.5 XPS spectra of (a) survey spectrum, (b) Ti 2*p*; (c) O 1*s*; and (d) N 1*s* for TNAs calcined at 450 ℃ for 2 h

3.5 Results of photocatalytic activity

In order to investigate the photocatalytic activity of double layer TNAs, degradation results of methyl orange dye under UV light as a function of time were shown in Fig.6. Three different TNAs, TNAs formed in 0.5 wt% HF solution, double-layere TNAs formed by anodizing in 0.5 wt% HF solution for 20 min, and

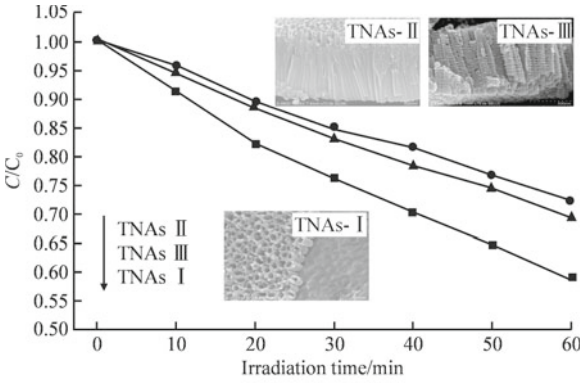

Fig.6 Kinetic of MO degradation for different TNAs(The insets show the cross-sectional images of samples used for photocatalysis experiment)

then in 0.27 M ammonium fluoride in formamide containing 3% volume water for 5 min, and TNAs formed in glycerol and water (50:50 vol%) +0.5 wt% NH_4F electrolyte had been studied. These three different TNAs hereafter were designated as TNAs-I, TNAs-II and TNAs-III, respectively. The lengths of three samples were 350 nm, 1 μm (the first layer of 200 nm and 800 nm for the second layer) and 900 nm. MO was slowly degraded under 300 W UV light. After 1 h irradiation, about 45% MO was degraded by TNA-I while TNA-II and TNA-III showed even poorer degradation ability, and less than 30% MO was degraded. The degradation percent of MO obeyed the following order: TNAs-I＞TNAs-III＞TNAs-II. The double-layer TNAs showed the lowest reaction rate under UV irradiation. This result indicated that the photodegradation ability was not related with the length of nanotube arrays.

The apparent rate constant (k_{app}) was chosen as the basic kinetic parameter for the different TNAs. The apparent first order kinetic equation:

$$\ln\left(\frac{C_0}{C}\right) = k_{app} \times t \tag{1}$$

The equation was used to fit experimental data in Fig.6, where C was the concentration of the MO

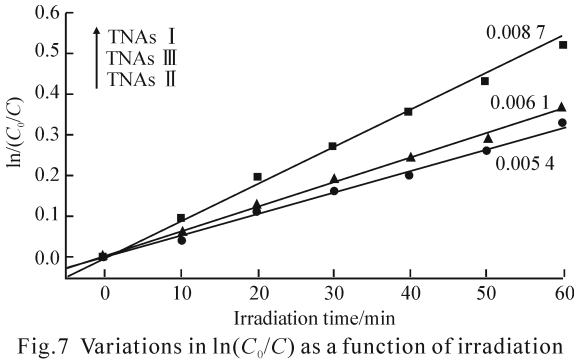

Fig.7 Variations in $\ln(C_0/C)$ as a function of irradiation time and linear fits of different TNAs

solution at t, and C_0 is the initial concentration of MO at t=0[22]. The variations in ln(C_0/C) as a function of irradiation time were given in Fig.7. The k_{app} decreased in the order: TNAs-I＞TNAs-III＞TNAs-II.

4 Conclusions

The results of the present work showed that double-layer TNAs could be obtained successfully by two-step anodization under different electrochemical conditions. The first layer grown in the HF solution did the favor of the formation of the second layer and at the same time, it protected the second layer from excessive chemical etching. The thickness of second layer corresponded to the anodization time, the increasing of which would lead to the excessive etching on the first layer.

References

[1] C A Grimes, K G Ong, O K Varghese, *et al.* A Sentinel Sensor Network for Hydrogen Sensing[J]. *Sensors*, 2003, 3: 69-82

[2] E Sennik, Z Colak, N Kilinc, *et al.* Synthesis of Highly-ordered TiO_2 Nanotubes for a Hydrogen Sensor[J]. *Int. J. Hydrogen Energy*, 2010, 35: 4 420-4 427

[3] Z H Zhang, M F Hossain, T Takahashi. Photoelectrochemical Water Splitting on Highly Smooth and Ordered TiO_2 Nanotube Arrays for Hydrogen Generation[J]. *Int. J. Hydrogen Energy*, 2010, 35: 8 528-8 535

[4] K Shankar, G K Mor, H E Prakasam, *et al.* Self-Assembled Hybrid Polymer-TiO_2 Nanotube Array Heterojunction Solar Cells[J]. *Langmuir*, 2007, 23: 12 445-12 449

[5] K Shankar, J Bandara, M Paulose, *et al.* Highly Efficient Solar Cells using TiO_2 Nanotube Arrays Sensitized with a Donor-Antenna Dye[J]. *Nano Lett*., 2008, 8(6): 1 654-1 659

[6] Y B Liu, B X Zhou, B T Xiong, *et al.* TiO_2 Nanotube Arrays and TiO_2 -nanotube-array Based Dye-sensitized Solar Cell[J]. *Chin. Sci. Bull*., 2007, 52(12): 1 585-1 589

[7] R Wang, K Hashimoto, A Fujishima, *et al.* Photogeneration of Highly Amphiphilic TiO_2 Surfaces[J]. *Adv. Mater*., 2008, 10(2): 135-138

[8] A Kodama, S Bauer, A Komatsu, *et al.* Bioactivation of Titanium Surfaces Using Coatings of TiO_2 Nanotubes Rapidly Pre-loaded with Synthetic Hydroxyapatite[J]. *Acta Biomaterialia*, 2009, 5: 2 322-2 330

[9] S C Roy, M Paulose, C A Grimes. The Effect of TiO_2 Nanotubes in the Enhancement of Blood Clotting for the Control of Hemorrhage[J]. *Biomaterials*, 2007, 28: 4 667-4 672

[10] D W Gong, C A Grimes, O K Varghese, *et al.* Titanium Oxide Nanotube Arrays Prepared by Anodic Oxidation[J]. *J. Mater. Res*., 2001, 16(12): 3 331-3 334

[11] J M Macak, H Tsuchiya, A Ghicov, *et al.* TiO_2 Nanotubes: Self-organized Electrochemical Formation, Properties and Applications[J]. *Curr. Opin. Solid State Mater. Sci*., 2007, 11: 3-18

[12] Q Y Cai, M Paulose, O K Varghese, *et al.* The Effect of Electrolyte Composition on the Fabrication of Self-organized Titanium Oxide Nanotube Arrays by Anodic Oxidation[J]. *J. Mater*., 2005, 20(1): 230-236

[13] J M Macak, H Tsuchiya, P Schmuki. High-Aspect-Ratio TiO_2 Nanotubes by Anodization of Titanium[J]. *Angew. Chem. Int. Ed*., 2005, 44: 2 100 -2 102

[14] C J Carstensen, H Foll. Crystal Orientation Dependence of Macropore Formation in *n*-Type Silicon Using Organic Electrolytes[J]. *Phys. Status Solidi. A*, 2000, 182(2): 601-606

[15] C J Carstensen, H Foll. Organic and Aqueous Electrolytes Used for Etching Macro-and Mesoporous Silicon[J]. *Phys. Status Solidi. A,* 2003, 197(1): 34 -38

[16] M Paulose, H E Prakasam, O K Varghese, *et al.* TiO_2 Nanotube Arrays of 1 000 μm Length by Anodization of Titanium Foil: Phenol Red Diffusion[J]. *J. Phys. Chem. C*, 2007, 11: 14 992-14 997

[17] Z Y Liu, X T Zhang, S Nishimoto, *et al.* Highly Ordered TiO_2 Nanotube Arrays with Controllable Length for Photoelectrocatalytic Degradation of Phenol[J]. *J. Phys. Chem. C*, 2008, 112: 253-259

[18] J M Macak, P Schmuki. Anodic Growth of Self-organized Anodic TiO_2 Nanotubes in Viscous Electrolytes[J]. *Electrochem. Acta*, 2006, 52: 1 258-1 264

[19] J M Macak, S Albu, D H Kim, *et al.* Multilayer TiO_2-Nanotube Formation by Two-Step Anodization[J]. *Electrochem. Solid-state Lett.*, 2007, 10(7): K28-K31

[20] S Lee, C Y Yun, M S Hahn, *et al.* Synthesis and Characterization of Carbon-doped Titania as a Visible-light-sensitive Photocatalyst[J]. *Korean J. Chem. Eng*., 2008, 25(4): 892-896

[21] T Horikawa, M Katoh, T Tomida. Preparation and Characterization of Nitrogen-doped Mesoporous Titania with High Specific Surface Area[J]. *Microporous Mesoporous Mater*., 2008, 110: 397-404

[22] J Matos, J Laine, J M Herrmann. Synergy Effect in the Photocatalytic Degradation of Phenol on a Suspended Mixture of Titania and Activated Carbon[J]. *Appl. Catal., B: Environ*., 1998, 18(3-4): 281-291